

UnPaSt: unsupervised patient stratification by differentially expressed biclusters in omics data

Michael Hartung^{1*}, Andreas Maier^{1*}, Fernando Delgado-Chaves¹, Yuliya Burankova^{1,2}, Olga I. Isaeva³, Fábio Malta de Sá Patroni⁴, Daniel He⁵, Casey Shannon⁵, Katharina Kaufmann¹, Jens Lohmann¹, Alexey Savchik⁶, Anne Hartebrodt⁷, Zoe Chervontseva¹, Farzaneh Firoozbakht¹, Niklas Probul¹, Evgenia Zotova⁸, Olga Tsoy¹, David B. Blumenthal⁷, Martin Ester^{9,10}, Tanja Laske¹, Jan Baumbach^{1,11†}, Olga Zolotareva^{1,12†}.

¹ *Institute for Computational Systems Biology, University of Hamburg, Albert-Einstein-Ring 10, Hamburg, Germany*

² *Chair of Proteomics and Bioanalytics, TUM School of Life Sciences, Technical University of Munich, Freising, Germany*

³ *Division of Tumor Biology & Immunology, Netherlands Cancer Institute, Plesmanlaan 121, Amsterdam, the Netherlands*

⁴ *University of Campinas, Campinas, Brazil*

⁵ *University of British Columbia, Vancouver, Canada*

⁶ *ACMetric, Amsterdam, the Netherlands*

⁷ *Friedrich-Alexander-Universität Erlangen-Nürnberg, Erlangen, Germany*

⁸ *Altius Institute for Biomedical Sciences, Seattle, United States.*

⁹ *Simon Fraser University, Burnaby, Canada*

¹⁰ *Vancouver Prostate Centre, Vancouver, Canada*

¹¹ *Department of Mathematics and Computer Science, University of Southern Denmark, Odense, Denmark.*

¹² *Data Science in Systems Biology, TUM School of Life Sciences, Technical University of Munich, Freising, Germany*

* - joint first author

† - joint last author

Abstract

Most complex diseases, including cancer and non-malignant diseases like asthma, have distinct molecular subtypes that require distinct clinical approaches. However, existing computational patient stratification methods have been benchmarked almost exclusively on cancer omics data and only perform well when mutually exclusive subtypes can be characterized by many biomarkers. Here, we contribute with a massive evaluation attempt, quantitatively exploring the power of 22 unsupervised patient stratification methods using both, simulated and real transcriptome data.

From this experience, we developed UnPaSt (<https://apps.cosy.bio/unpast/>) optimizing unsupervised patient stratification, working even with only a limited number of subtype-predictive biomarkers. We evaluated all 23 methods on real-world breast cancer and asthma transcriptomics data. Although many methods reliably detected major breast cancer subtypes, only few identified Th2-high asthma, and UnPaSt significantly outperformed its closest competitors in both test datasets. Essentially, we showed that UnPaSt can detect many biologically insightful and reproducible patterns in omic datasets.

Main

Introduction

Historically, classifications of human diseases are based on symptoms and affected organs. Exploration of large clinical and omics data revealed that many diseases are heterogeneous at the molecular level, i.e., represent groups of disorders with similar manifestations, but different mechanisms and etiologies. Molecular heterogeneity is well known for malignancies, which are being subdivided into clinically relevant subtypes based on omics data¹. Nowadays, with growing evidence, it is becoming increasingly clear that some non-malignant diseases also consist of molecular subtypes²⁻⁶. This unaccounted-for disease heterogeneity may explain the drug inefficacy in some patients⁷ and the low success rate in translating preclinical results into clinical applications⁸. Additionally, the presence of distinct subtypes in datasets can create interference in the downstream analysis and impede the elucidation of disease mechanisms.

To achieve an unbiased and purely data-driven perspective on disease subtypes, it is common to stratify patients in an unsupervised fashion. Traditionally, this problem is approached by conventional clustering and factorization methods such as k-means, hierarchical clustering, or non-negative matrix factorization (NMF) and related methods⁹⁻¹¹. These methods have helped to discover many disease subtypes and have been particularly successful in transcriptome-based stratification of cancers^{12,13}, where molecular subtypes are well-differentiated by a large number of differentially expressed genes. In this study we show that conventional clustering methods do not perform well when the number of subtype-specific biomarkers is small compared to the dimensionality of clustered objects, or when the subtypes are not mutually exclusive and some samples belong to multiple subtypes.

Biclustering methods search for subsets of rows and columns in a two-dimensional matrix, such that the corresponding submatrices express a specific pattern. Because many biclustering methods are capable of identifying intersecting submatrices, they can discover overlapping patterns¹⁴⁻¹⁶. Unlike conventional clustering methods, which compare objects taking into account all input features, biclustering methods compare objects in subspaces of some selected features and therefore can still be effective when the number of subtype-specific biomarkers is small and the majority of features are irrelevant for classification (Figure 1).

Despite these advantages, biclustering methods are largely overlooked in recent patient stratification benchmarks¹⁷⁻²². These studies are primarily focused on the methods designed specifically for multi-omics data and performing data integration together with sample clustering, although many established molecular classifications of human diseases are defined solely on transcriptome data^{2,12,23,24}. Since patient stratification based on multi-omics is computationally expensive, with some exceptions^{17,18}, the methods were tested only with varying expected number of clusters while the other parameters were not tuned^{18,20,21}. Moreover, most popular stratification methods were almost exclusively evaluated on cancer data with the pronounced differences between subtypes¹⁸⁻²² and their performance on non-malignant diseases remains unexplored, despite the growing evidence of their heterogeneity²⁻⁶.

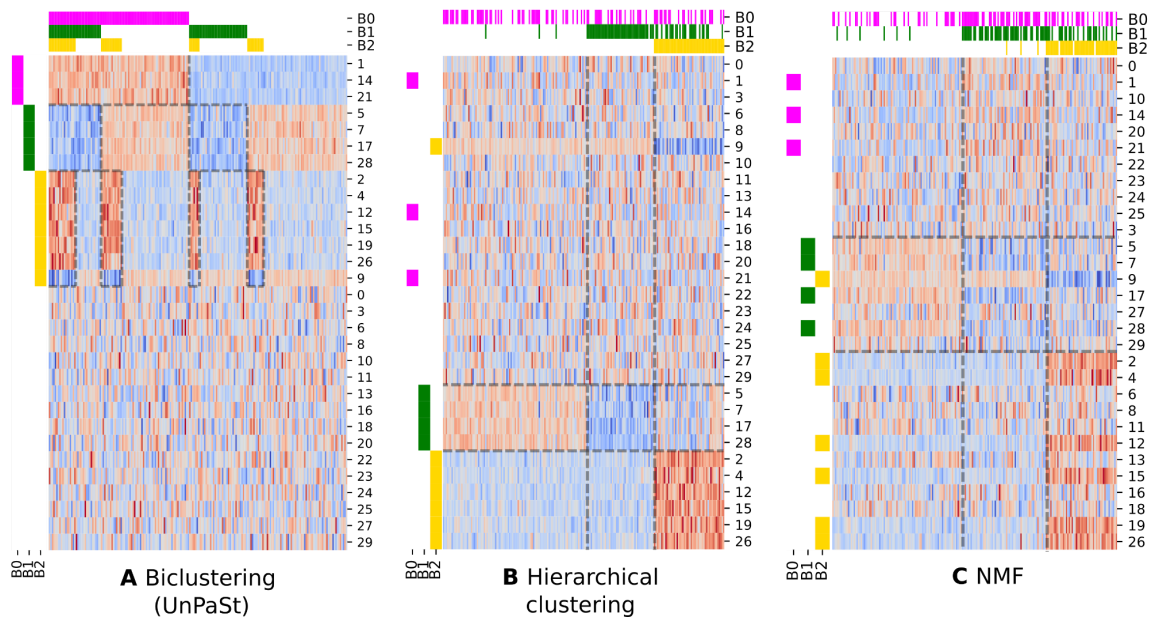


Figure 1. The advantage of biclustering (A) over popular unsupervised learning methods, agglomerative hierarchical clustering of rows and columns (B) and negative matrix factorization (NMF, C) on the example of a toy data matrix, consisting of 30 rows and 200 columns and including three differentially expressed biclusters (B0,B1,B2). Color bars on heatmaps' borders show row and column membership in true biclusters. Clusters and biclusters identified by each method are shown with dashed frames. The expected number of clusters was set to 3 for hierarchical clustering and NMF. UnPaSt was applied with enabled detection of bidirectional biclusters. All other parameters of each method were set to default values.

To overcome these limitations and to provide a comprehensive quantitative review on patient stratification methods performances, in this study, we benchmark a diverse spectrum of approaches for unsupervised patient stratification, including rarely used biclustering methods. Firstly, we focus on the methods' capabilities to *de novo* discover known molecular subtypes, and do not solely rely on proxy performance measures, such as associations with clinical features. To achieve a more complete view on methods' capabilities, we have not limited this study to testing methods only with default parameter settings but performed parameter optimization. Moreover, in addition to the breast cancer subtyping problem addressed in most similar works, we further applied the methods to stratification of patients with asthma, a common disease in which molecular subtypes are defined only by a few biomarkers².

While the majority of tested methods confidently detected frequent non-overlapping subtypes distinguished by multiple biomarkers in real and simulated data, their performance quickly dropped when the number of subtype-specific biomarkers decreased. Although some biclustering methods outperformed popular patient stratification methods in complex scenarios including overlapping sample clusters with limited number of biomarkers, their overall performance was not high. The reason for this deficiency might be that the patterns searched by many biclustering methods are more consistent with differential co-expression, while disease subtypes are frequently defined based on differential expression. This consideration prompted us to develop UnPaSt (<https://apps.cosy.bio/unpast/>), a novel method for unsupervised patient stratification, which is targeted specifically at differentially expressed biclusters, and to benchmark it against 22 popular patient stratification methods (Table 1) on real transcriptome and simulated datasets. In the concluding section of the

paper, we demonstrate the utility of UnPaSt for the analysis of other types of omics and multi-omics datasets.

method	type	overlapping sample clusters	extracts biomarkers	requires the number of clusters	deterministic algorithm
UnPaSt	Biclustering	yes	yes	no	no
QUBIC ²⁵		yes	yes	upper limit	yes
ISA2 ²⁶		yes	yes	upper limit	no
FABIA ²⁷		yes	yes	yes	no
COALESCE ²⁸		yes	yes	no	yes
BiMax ²⁹		yes	yes	yes	yes
Plaid ³⁰		yes	yes	upper limit	no
NMF ³¹	Factorization	no	yes	yes	no
sparse PCA ³²		no	yes	yes	no
MOFA2 ³³		no	no	yes	no
moCluster ³⁴		no	no	yes	yes
iClusterPlus ³⁵		no	no	yes	no
Affinity propagation (AP) ³⁶	Clustering	no	no	no	no
Bisecting K-Means ³⁷		no	no	yes	no
BIRCH ³⁸		no	no	yes	yes
DBSCAN ³⁹		no	no	no	yes
GMM		no	no	yes	no
Hierarchical clustering (HC) ⁴⁰		no	no	yes	yes
K-means		no	no	yes	no
MCLUST ⁴¹		no	no	yes	no
MeanShift ⁴²		no	no	no	yes
Mini-batch k-means		no	no	yes	no
Spectral clustering ⁴³		no	no	yes	no

Table 1. Comparison of the tested methods regarding unsupervised patient stratification.

Evaluation strategies

Although solid molecular classifications are established for some diseases, evaluating patient stratification results remains a challenging task. Among the approaches used in previous studies¹⁷⁻²², three strategies can be distinguished: direct estimation of method performances through the comparison of the predicted subtypes with the known ones by (i) using simulated data, (ii) using real data, or (iii) assessing method performances using proxies, such as association between predicted subtypes and clinical features. However, all three approaches might give biased performance estimates. Superior method performance in a synthetic data benchmark does not necessarily guarantee that this method will work equally well in more complex real-world scenarios⁴⁴. Correctly identified molecular subtypes may not necessarily demonstrate distinct clinical features, e.g. differential survival, drug response, or available metadata may be incomplete. Real data might contain many biologically meaningful patterns not related to known disease subtypes (e.g. unknown disease subtypes, sex-specific gene expression) or experimental artifacts (e.g. batch effects, contaminations), hindering the discrimination between actual true and false positives. Moreover, traditional clustering performance measures, such as F1 or adjusted Rand Index (ARI), assuming that the entire population of patients is divided into disjoint sample subsets, are not applicable for evaluation of biclustering results that contain many overlapping sample clusters. To enable performance estimation for overlapping sample clusters and to reduce the influence of unaccounted heterogeneity on performance estimates, we calculated the sum of weighted ARIs computed for each known subtype and its statistically significant best match among all identified sample clusters or biclusters (Methods).

Another challenge for the performance evaluation of patient stratification tools is the selection of the optimal method parameters. Since our previously published results suggest that the performance of many biclustering tools can be largely improved by proper parameter selection⁴⁴, in this work we used grid search to tune methods' parameters. In real-world conditions, however, parameter tuning by optimizing an external performance metric cannot be implemented due to the absence of ground truth. Therefore, this work does not provide the recipes for parameter tuning, but rather evaluates the necessity of parameter tuning for the compared methods. To control for overfitting, after tuning methods' parameters on one dataset, we additionally evaluated it on another independently created dataset with the same features and clinical characteristics. Regardless of the overfitting control, this validation reduces the chance of capturing dataset-specific perturbations emerging due to the sampling bias or batch effects instead of the actual disease subtypes.

Results

UnPaSt Algorithm

To unlock the potential of biclustering for the identification of disease subtypes, we developed UnPaSt, a novel algorithm to identify differentially expressed biclusters. As input, UnPaSt accepts a two-dimensional matrix of S samples and F features (e.g. gene expressions). UnPaSt identifies subsets of features F_1, \dots, F_i, \dots , used to split S into two well-separated subsets with distinct values for each j -th feature $f_j \in F_i$. For simplicity, we will further refer to a smaller sample set S_{F_i} as “bicluster” sample set and a bigger sample

set $\overline{S_{F_i}} = S \setminus S_{F_i}$ as the “background” sample set (Figure 2A). Such biclusters $B_i = (F_i, S_{F_i})$ in transcriptome data may correspond to sample sets S_{F_i} that over- or under-express a certain pathway F_i . Because bicluster and background sample sets are not defined in the input and should be identified jointly with the feature subsets that differentiate them, this problem is related to unsupervised formulation of the differential expression analysis task. To highlight this, we will further refer to biclusters identified by UnPaSt as *differentially expressed biclusters*. Of note, UnPaSt does not guarantee that each feature $f_j \in F_i$ is statistically significantly differentially expressed in S_{F_i} samples compared to $\overline{S_{F_i}}$. Each bicluster may consist of exclusively over- or under-expressed features, or can be of mixed-type and include features diverging from the background in both directions (Figure 2B).

UnPaSt identifies differentially expressed biclusters in a two-dimensional matrix in three consequent steps (Figure 2D-E). In the first step, for each feature f_j (e.g., gene expression), all samples are split into two subsets with higher and lower values (Figure 2D). Unlike some other methods setting a fixed threshold^{29,45}, UnPaSt employs clustering to optimize the separation of the samples into two groups S_{f_j} and $\overline{S_{f_j}}$ representing bicluster and background sample sets (Figure 2F). Bicluster and background sets are defined such that $|S_{f_j}| < |\overline{S_{f_j}}|$, or assigned randomly when $|S_{f_j}| = |\overline{S_{f_j}}|$. Currently, users can choose between 2-means clustering, hierarchical clustering, and a mixture of two Gaussians, converting each feature into a binary vector where ones are assigned to samples from the bicluster set S_{f_j} . Then, UnPaSt selects features defining well-separated sample subgroups of at least n_s samples ($n_s = 5$ by default), and thus indicating molecular heterogeneity, potentially being most relevant for patient stratification. The quality of sample set S_{f_j} separation from the background $\overline{S_{f_j}}$ based on j -th feature values is measured by the signal-to-noise ratio (SNR):

$$SNR(f_j, S_{f_j}) = \frac{|\mu_{f_j, S_{f_j}} - \mu_{f_j, \overline{S_{f_j}}}|}{\sigma_{f_j, S_{f_j}} + \sigma_{f_j, \overline{S_{f_j}}}},$$

where $\mu_{f_j, S_{f_j}}$ and $\mu_{f_j, \overline{S_{f_j}}}$ are mean values, and $\sigma_{f_j, S_{f_j}}$ and $\sigma_{f_j, \overline{S_{f_j}}}$ are standard deviations of feature f_j in bicluster S_{f_j} and background $\overline{S_{f_j}}$ sample sets respectively.

SNR values computed for all features cannot be directly compared because the variance of estimated SNRs depends on the sizes of S_{f_j} and $\overline{S_{f_j}}$ which vary across features. Therefore, to distinguish between well- and poorly binarized features, UnPaSt compares each observed $SNR(f_j, S_{f_j})$ with the distribution of SNR values obtained by splitting a standard normal distribution into two groups of the same size as $|S_{f_j}|$ and $|\overline{S_{f_j}}|$ $\max(10000, \frac{10}{p})$ times (where p is a user defined p -value threshold). Based on this null model, empirical binarization p -values are assigned to all features, and only features with p -values exceeding a user-defined threshold are passed to the second phase of the workflow (Figure 2E).

In the second step, binarized features defining well-separated sample sets are clustered into modules based on the similarity of their binary profiles (Figure 2D), i.e., the resulting modules include features that distinguish similar sets of samples. Users can choose between Louvain[[10.1088/1742-5468/2008/10/P10008](https://doi.org/10.1088/1742-5468/2008/10/P10008)] and WGCNA⁴⁶ methods for feature clustering and specify method parameters to control clustering sharpness. Importantly, both methods do not require specifying the expected number of clusters but determine it automatically. Relying on different assumptions about the topology of similarity networks, Louvain clustering maximizes modularity⁴⁷ when dissecting pairwise similarity networks into clusters, whereas WGCNA converts the similarity network into a topological overlap matrix and selects a cutoff resulting in a network topology best fulfilling the scale-free property⁴⁸. This clustering is performed either for all that passed binarization at once, or separately for the two groups of features that define sample sets with under- or over-expression. Although the first approach allows finding mixed biclusters and “rescuing” otherwise not clustered individual features that are anti-correlated with all other features in a bicluster (like e.g. transcriptional repressors), UnPaSt demonstrated slightly higher performance when detecting over- and under-expressed biclusters independently.

In the third step, differentially expressed biclusters $B_i = (F_i, S_{F_i})$ are constructed from each module consisting of at least two features (Figure 2E). For that, samples are split into two clusters S_{F_i} and $\overline{S_{F_i}}$ in a subspace of the feature set F_i using the same binarization method used in the first step. As done for individual features, the SNR is computed for each bicluster by taking the average across features. As a post-processing step, to ensure that the identified biclusters capture statistically significant differential expression patterns, the UnPaSt package allows to run *limma*⁴⁹ for each $B_i = (F_i, S_{F_i})$, testing all features for significance of differential expression between S_{F_i} and $\overline{S_{F_i}}$, and selecting significantly differentially expressed features given user-defined thresholds for log2-fold-change and adjusted p -values.

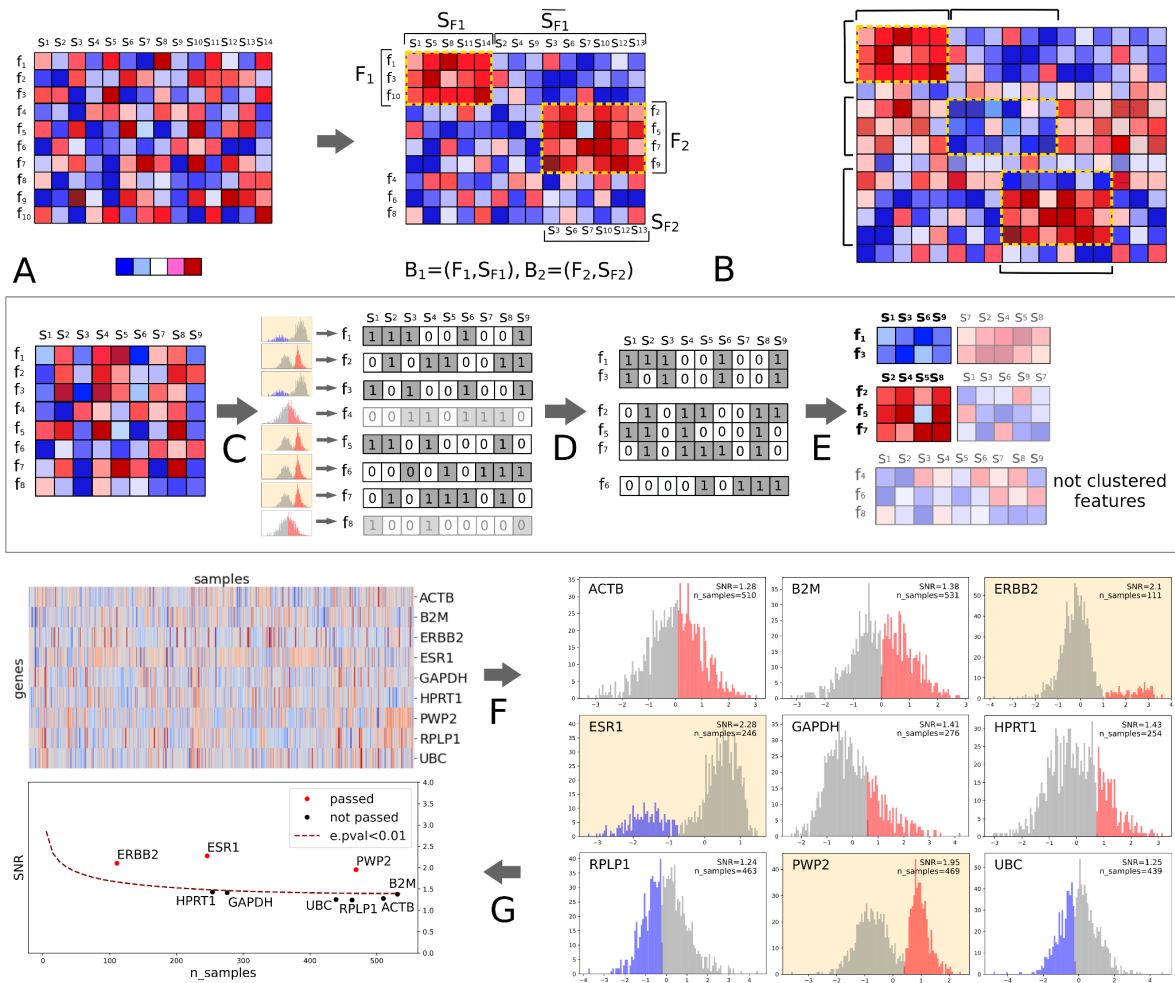


Figure 2. A. Input and output of UnPaSt. Given a two-dimensional matrix (on the left), UnPaSt identifies submatrices consisting of features and samples (on the right), such that these features are differentially abundant in corresponding samples. **B. Types of differentially expressed biclusters.** A bicluster can contain features that are either over-expressed, under-expressed, or a mix of both. **C-E. The UnPaSt workflow** on the example of a matrix with two biclusters. **C. Feature binarization.** Each individual feature vector turned into a binary vector where ones correspond to the smaller sample set. All features except f_4 and f_8 , whose binarization gave two poorly separated sample groups with low SNR, passed to the next phase. **D. Clustering of binarized features.** **E. Sample clustering.** To construct biclusters, samples are split into two sets based on the subset of features corresponding to each module. This results in two biclusters: one down-regulated and one up-regulated bicluster. Three features f_4, f_6, f_8 remain unclustered. **F-G: The UnPaSt approach to feature binarization** on the example of nine gene expressions in 1079 samples from TCGA-BRCA dataset (left panel). **F.** Expressions of well-known housekeeping genes ACTB, B2M, GAPDH, HPRT1, RPLP1, and UBC demonstrate unimodal bell-shaped distributions which are binarized using Ward's method with a threshold close to their medians. In contrast, known breast cancer biomarkers ESR1, ERBB2, and PWP2 show bimodal or heavy-tailed distributions and define two well-distinguishable sample sets each. The smaller sample set will be used as a bicluster seed and is highlighted with red or blue, depending on whether it over- or under-expresses this gene compared to the background (larger sample set, colored gray) **G.** SNRs computed for each of the nine features are compared with the empirical distributions of SNRs obtained by binarizing standard normal distributions. Only ESR1, ERBB2, and PWP2 empirical p-values pass the threshold of 0.01 (red dashed line).

Benchmark on simulated data

Before applying the methods to real data for which the complete ground truth is unavailable, we tested their ability to identify subtypes in artificial datasets consisting of 200 samples and 10,000 features (see Figure 3A, Supplementary Figure S1, and Methods for details). Because certain data properties can greatly influence the actual complexity of the stratification problem, we simulated three scenarios with growing complexity (A,B,C) and varied the number of subtype-specific biomarkers from 5 to 50 and 500 in each scenario. In scenario A, four non-overlapping clusters consisting of 5%-50% of all samples simulated four mutually exclusive disease subtypes. In scenarios B and C, sample clusters were allowed to overlap, i.e. each sample could be assigned to many clusters. To investigate whether the presence of other patterns in the data complicates the detection of simulated disease subtypes, in scenario C, four 500-feature co-expression modules not correlated with the subtypes were added to each data matrix. Method performance was measured as the sum of the ARIs computed for each simulated subtype and its best match among all identified sample clusters, weighted proportionally to the subtype prevalence (see Methods for details).

As shown in Figure 3B, the best performance demonstrated by all methods except UnPaSt dropped with the decrease of subtype-specific biomarker counts in all scenarios. With a number of biomarkers as low as five, only several methods were able to detect sample clusters strongly and significantly overlapping with the true sample clusters. Also, for conventional clustering and factorization methods, sample clustering was more challenging when the clusters were overlapping and the data contained additional co-expression modules not related to sample clusters, as it is likely to happen in real-world omics data. Simultaneously, the performance of some biclustering methods including UnPaSt did not reduce much in scenarios B and C compared to scenario A with the same number of biomarkers.

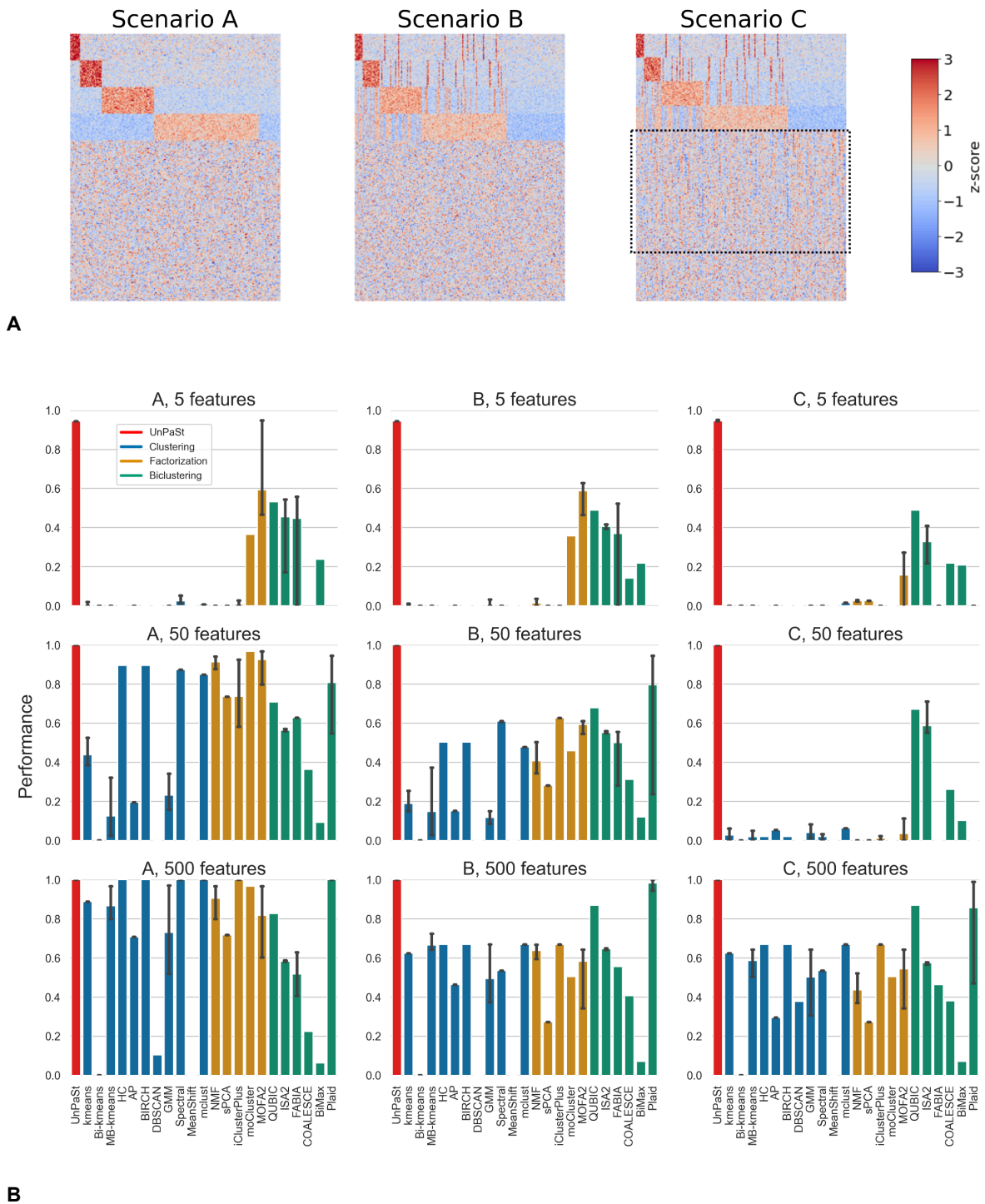


Figure 3. A. The heatmaps for standardized datasets from scenarios A, B, and C with 500-feature subtypes (only 3000 background features are shown). In scenario C, the dashed frame highlights modules of co-expressed genes. **B.** The performances of UnPaSt and other methods on simulated data, with parameters resulting in the best average performance over all nine datasets. The nine datasets were obtained as a combination of three scenarios (A, B, C) and three sizes of subtype-specific feature sets (5, 50, 500), each dataset consisted of 10000 features in 200 samples, and four sample clusters (see Methods and Supplementary Figures S1 and S2 for details). In scenario A, the four subtypes were mutually exclusive and did not overlap in samples. In scenarios B and C, the subtypes were not mutually exclusive and each sample

could belong to none or multiple subtypes. In Scenario C, besides four subtype-specific signatures, four modules of 1000 correlated features each (average within-module Pearson's correlation of about 0.5) were added to the background. Method performance was calculated as the sum of the ARI computed for each simulated subtype and its statistically significant best match among all sample clusters identified by this method, weighted proportionally to the subtype prevalence (see Methods for details). Runs that did not terminate successfully were excluded from this evaluation.

Unsupervised identification of breast cancer subtypes

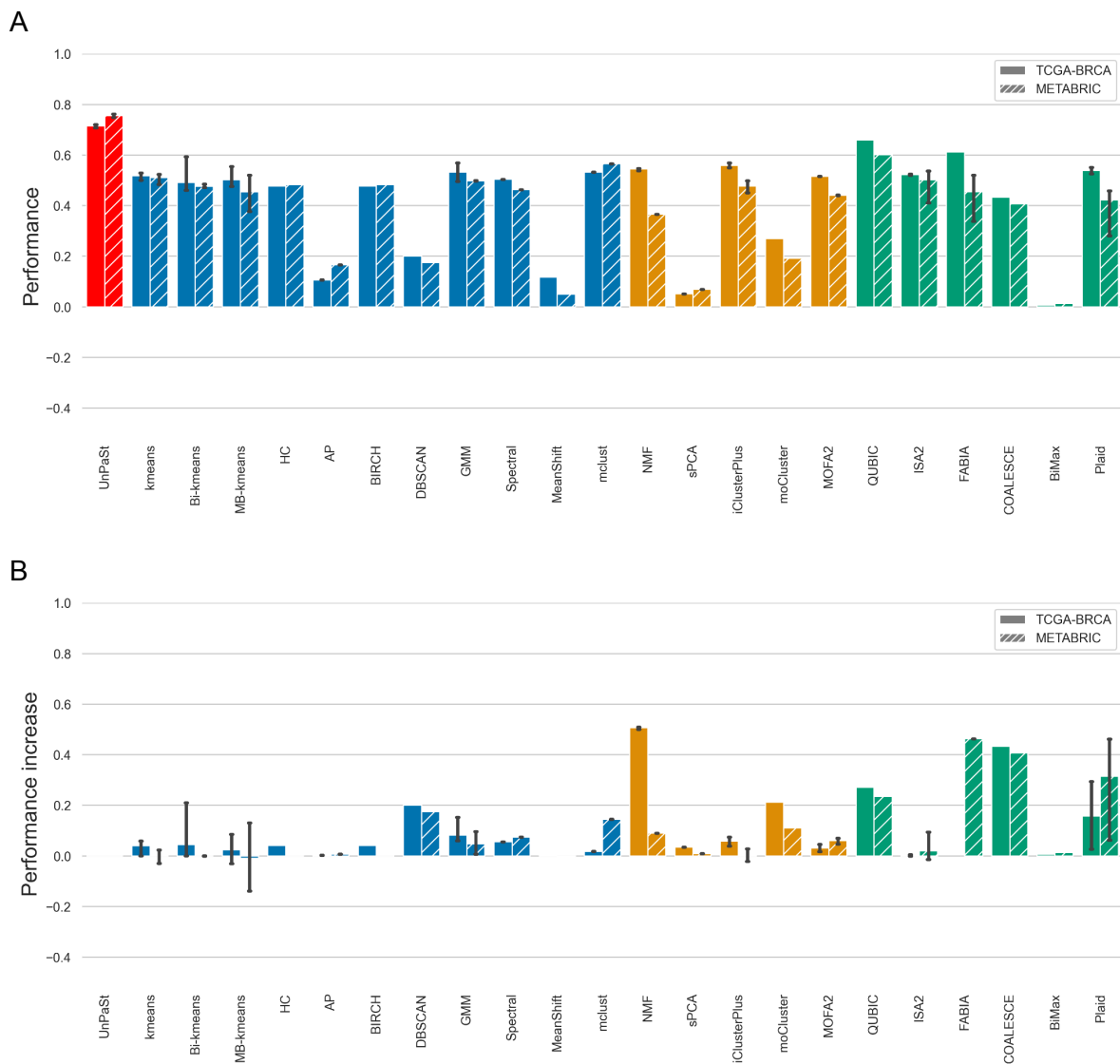
Breast cancer was one of the first diseases for which a molecular classification based on gene expression was proposed²³. Initially, four molecular subtypes (Basal-like, HER2-enriched, Luminal, and Normal-like) were identified by hierarchical clustering of 65 tumor samples based on expressions of 1753 genes selected by the researchers²³. Later, the Luminal subtype was further subdivided into two subgroups with distinct proliferation rates (Luminal A and B)⁵⁰ and other molecular subtypes of breast cancer (e.g. claudine-low^{51,52}, neuroendocrine^{53,54}) were defined. Now, the standard for breast cancer subtyping is the PAM50 classifier, which determines subtypes by expressions of 50 genes⁵⁵.

To evaluate UnPaSt and its baselines, we applied them to two large breast cancer datasets, TCGA-BRCA⁵⁶ and METABRIC⁵⁷ consisting of 1089 and 1904 tumor expression profiles, respectively. Resulting sample clusters were matched with subtypes defined by the supervised PAM50 classifier and overall method performance was calculated as the weighted sum of ARI values of known subtypes and their best matches among predicted clusters (Methods). Because method performances depend on set parameters, each method was run multiple times with varying parameter combinations (Supplementary Table S1). To avoid parameter overfitting for a specific dataset, we compared overall method performances with parameter combinations having the best average rank across all combinations tested in both datasets (Fig. 4A). Among all tested methods, UnPaSt demonstrated the highest overall performance in unsupervised detection of breast cancer subtypes (0.72 (TCGA-BRCA) - 0.76 (METABRIC) achieved by UnPaSt on average in five runs, compared to 0.66 (TCGA-BRCA) - 0.60 (METABRIC) reached by the second best method, QUBIC). Moreover, biclusters produced by UnPaSt matched with sample sets defined as IHC-confirmed overexpression or ER, HER2, and PR better than clusters or biclusters identified by any other (Supplementary Figure S4). Compared to individual breast cancer subtypes, UnPaSt biclusters were the best matching for the Luminal subtype, and the second or third best matching for the Basal and HER2-enriched subtypes, slightly inferior to the findings of other biclustering methods. Normal-like and Claudin-low subtypes, as well as Luminal A and B as isolated subgroups, were hardly detectable by all tested methods. Interestingly, the best matches for Normal-like and Claudin-low subtypes were detected in both dataset by other biclustering tools, ISA2 and COALESCE, respectively (Supplementary Figure S4).

To quantify the effect of parameter tuning, we calculated performance increase after parameter optimization in comparison to the performance with default settings for each method (Fig. 4B) Notably, only one clustering, two factorization, and four biclustering methods did heavily benefit from parameter optimization and the performance of the majority of conventional clustering methods improved only slightly in this benchmark. UnPaSt, ISA2, COALESCE, and iCluster+ demonstrated comparably high performance with all or most tested parameter combinations (Supplementary Figure S3), which is advantageous in

real-world scenarios when the ground truth is unavailable and parameter tuning is challenging.

While assessing the performance of patient stratification methods on breast cancer data, it is important to consider that the breast cancer dataset from TCGA represents one of the most popular benchmarks for these methods and could have been used in the early stages of their development, which might predispose them to demonstrate high performance in these tests. Furthermore, the most prevalent breast cancer subtypes have very distinct expression profiles and can be easily differentiated by hundreds of biomarkers, which may not be the case for other diseases (Supplementary Figure S5). Therefore, to get a more comprehensive method performance assessment, we further tested the methods on asthma data, representing an example of a non-malignant but heterogeneous disease with less distinct molecular subtypes. Because in real-world scenarios parameter optimization with the use of ground truth is not feasible, we omitted it in the consequent tests and applied each method only twice, with default parameters and parameters tuned on breast cancer data (i.e. having the best average rank on TCGA-BRCA and METABRIC datasets), further referred to as "optimized parameters".



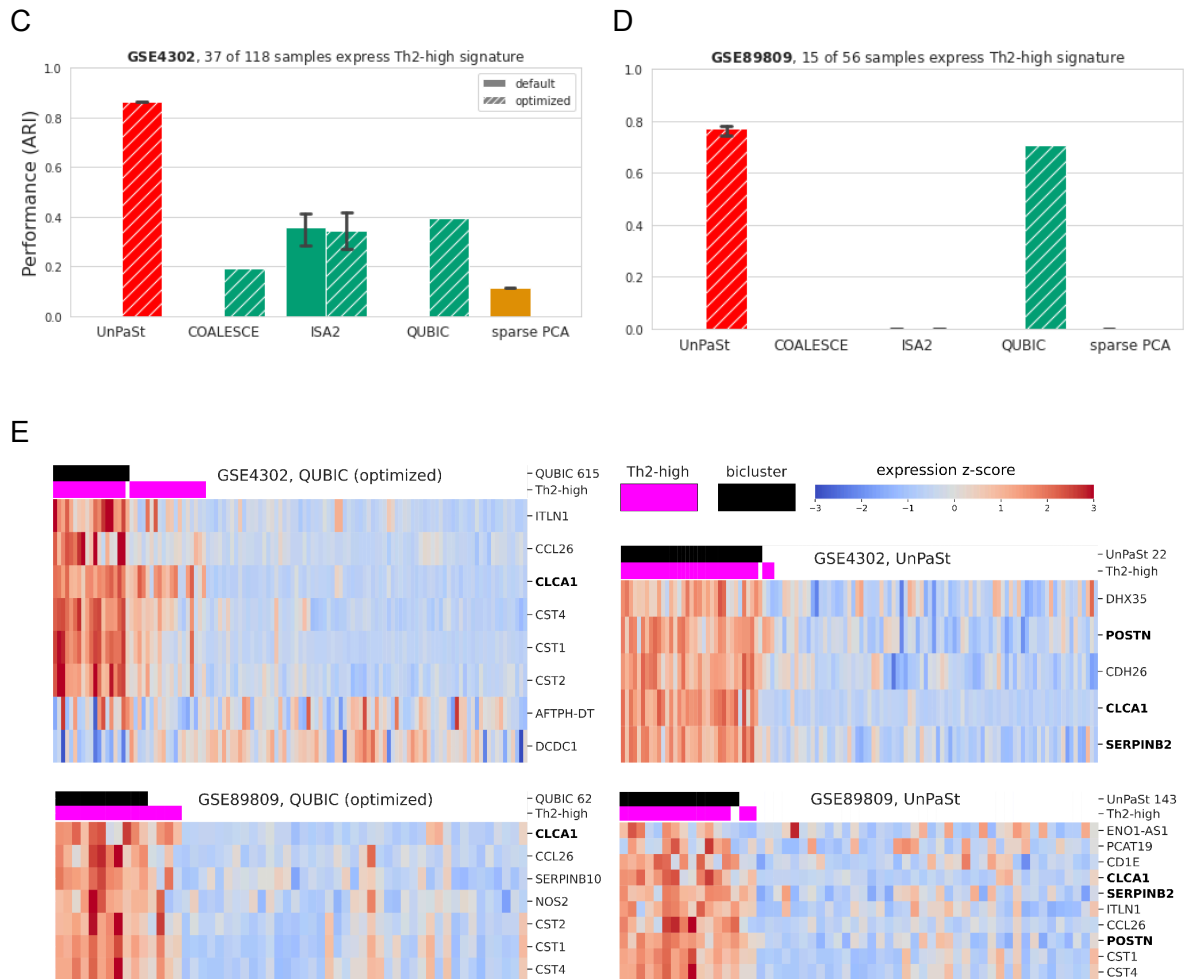


Figure 4. Identification of the known molecular subtypes in asthma and breast cancer.

A. The performances of patient stratification methods demonstrated in tests on METABRIC and TCGA-BRCA datasets, with optimized parameters having minimal average rank for both datasets. **B.** Performance gain after parameter optimization in comparison to the performance with default settings. COALESCE did not terminate after one week running with default parameter settings and assumed to demonstrate zero performance. UnPaSt is shown to have zero performance increase since the optimized parameters used in this study were set as defaults. **C-E.** Identification of Th2-high asthma with default and optimized parameters in GSE4302² and GSE89809⁵⁸ datasets. Only the methods whose results obtained on GSE4302 (**C**) and GSE89809 (**D**) datasets contained a statistically significant best match for Th2-high asthma sample subset are shown. Each method was tested with default parameters and parameters optimized on breast cancer data. UnPaSt and other non-deterministic methods were run five times with different seeds for each dataset and parameter combination. **E.** Biclusters identified by UnPaSt and its closest competitor QUBIC best matched the Th2-high asthma subsets in GSE4302 and GSE89809 cohorts. Each heatmap shows standardized expressions of bicluster genes (rows). Sample annotation above each heatmap specifies the membership of samples in the bicluster (black) and whether the sample is over-expressing the Th2 signature defined by three biomarkers (magenta), CLCA1, POSTN, and SERPINB2 (highlighted with bold text font). In both datasets, UnPaSt biclusters match Th2-high asthma more precisely than QUBIC biclusters. Since UnPaSt is a non-deterministic method, consensus biclusters from five independent runs are shown.

Unsupervised identification of Th2-high asthma

Asthma is a common inflammatory disorder of the respiratory system and many studies report its symptomatic and molecular heterogeneity^{59,60}. Woodruff et al. proposed to distinguish two molecular phenotypes of asthma defined by the level of T-helper 2

(Th2)-driven inflammation in bronchial epithelium²: “Th2-high” and “Th2-low” asthma. Further studies confirmed the presence of Th2 signature in a subset of asthma patients⁶¹, investigated its role in the pathology of asthma, and confirmed its clinical significance for treatment selection. Unlike breast cancer subtypes, only several biomarkers differentiate Th2-high and -low asthma subtypes, making their unsupervised discovery a challenging task. To examine whether the optimization of parameters on breast cancer data generally improved method performance or only overfitted the method specifically for breast cancer, we applied each method twice, with default parameters and the parameters optimized in the breast cancer benchmark.

The ARI of the sample splits corresponding to clusters best matching the Th2-high group and their complements in both datasets are shown in Figures 4C-D. Of all methods, only UnPaSt, COALESCE, QUBIC, ISA2, and sparse PCA identified sample sets significantly overlapping with the Th2-high subgroup defined as described in Woodruff et al. (see Methods for the details). No sample set output by any conventional clustering method overlapped the Th2-high group better than could be expected by chance (p -value cutoff of 0.05 after BH procedure was applied). Of all tested methods, only UnPaSt and QUBIC identified biclusters significantly overlapping Th2-high asthma in both datasets. In both cases, UnPaSt identified the Th2-high subset more precisely than QUBIC, as ARIs of 0.87 and 0.72-0.78 were achieved by UnPaSt, and 0.4 and 0.71 by QUBIC on GSE4302 and GSE89809 datasets, respectively. Importantly, UnPaSt biclusters best matching the Th2-high subset included all three biomarkers of Th2-high asthma (CLCA1, POSTN, SERPINB2), while QUBIC biclusters included only CLCA1 (Figure 4E).

UnPaSt reveals molecular heterogeneity beyond established disease classifications

Besides biclusters best matching known disease subtypes, UnPaSt discovered many other patterns with similar properties (size, SNR). Some of these biclusters may correspond to disease subtypes unaccounted for in the current molecular classifications or reflect biological variation unrelated to the disease mechanisms. To find biclusters that are more likely to correspond with biologically meaningful expression patterns rather than batch effects or contaminations, we (i) searched for similar biclusters in independent datasets, (ii) tested sample sets for associations with clinical variables and gene sets for overlap with known pathways or GO categories.

In GSE4302 and GSE89809 datasets consisting of expression from asthma patients and healthy controls, UnPaSt identified 81 and 104 biclusters, respectively, of which three pairs significantly (adjusted p -value < 0.05) and strongly (Jaccard similarity ≥ 0.25) overlapped in genes. The strongest overlap was observed for a pair of biclusters consisting of genes located on sex chromosomes and known to be differentially expressed in males and females (Fig. 5A,B). As expected, in GSE89809, this pattern perfectly separated samples obtained from male and female individuals (no information about donors' sex was provided in GSE4302). Two other strongly overlapping bicluster pairs were formed by biclusters 15 and 22 from GSE4302 matched to bicluster 143 from GSE89809. Biclusters 22 and 143 were already discussed in the previous section (Fig. 4E) as the best matches of the Th2-high subset. Bicluster 15 (Supplementary Figure S7) represented a subset of samples overexpressing Th2-high signature, and additionally included CCL26, CST1, CST2, CST4,

and ITLN1 previously linked with eosinophilia and Th2 response in asthma^{62,63}, suggesting that these genes might represent additional biomarker candidates of Th2-associated inflammation in asthma and beyond.

To examine biclusters not matched with Th2-high asthma, we tested them for association with other available variables. Bicluster 3 identified in GSE4302 included 14 of 16 samples received from the individuals who smoked (Fig. 5C, adjusted p-value < 1.8e-14). This 20-gene bicluster included ALDH3A1, CYP1B1, and GPX2 known to be up-regulated in airways in response to cigarette smoke⁶⁴, but had no significantly matching partner among biclusters found in GSE89809 data, because only one sample was obtained from a current smoker. Interestingly, in a biopsy obtained from this individual, these 20 genes are expressed at much higher levels than in any other sample (Fig. 5D). This finding demonstrates that the irreproducibility of some biologically meaningful associations in independent data may be attributed to data heterogeneity rather than the poor method performance.

In breast cancer datasets TCGA-BRCA and METABRIC, UnPaSt identified 209 and 180 differentially expressed biclusters, respectively, of which 75 pairs significantly (adjusted p-value < 0.05) overlapped in at least 2 genes (Supplementary Table S2) and 45 pairs had Jaccard similarity above 0.1. Of them, 34 of the 45 pairs were insignificantly or weakly associated with PAM50 subtypes (maximal ARI did not exceed 0.25 in any dataset). Although none of these replicated biclusters were significantly associated with overall survival in both datasets, they might demonstrate various aspects of cancer biology not directly related to the hormone receptor status. Figure 5E shows the five pairs of the matched biclusters found in TCGA-BRCA and METABRIC datasets selected based on the size of their shared gene sets. In particular, biclusters 100 and 163 (containing leptin, PLIN1, PLIN4, LPL, CIDEA, CIDEA, etc.) reflect the presence of adipocytes and adipogenesis which have a known role in breast cancer. Bicluster 64 (containing PSMD7) is related to immunoproteasome activity, which is relevant for efficient antigen presentation. Similarly, biclusters 36 and 22 contain many known cancer antigens (CSAG1, CSAG2, CTAG2, MAGE family members, PAGE1), which also may contribute to potential immune response. Biclusters 128 and 60 include genes related to interferon response (BATF2, IFIT1, IFIT2, IFIT3, ISG15, etc). Finally, biclusters 5 and 5 contain genes related to neuroendocrine biology: chromogranins A and B, NTF3, NTRK2, NTS, etc. These biclusters might be associated with neuroendocrine breast carcinoma (NEBC), a rare subtype of breast cancer accounting for 2-5% of all breast cancer cases. All these biological programs have a known role in breast cancer, however, their effects may be easily overlooked because of the stronger influences of hormone receptor presence and proliferation, which underscores the importance of biclustering tools in unveiling heterogeneity in biological data.

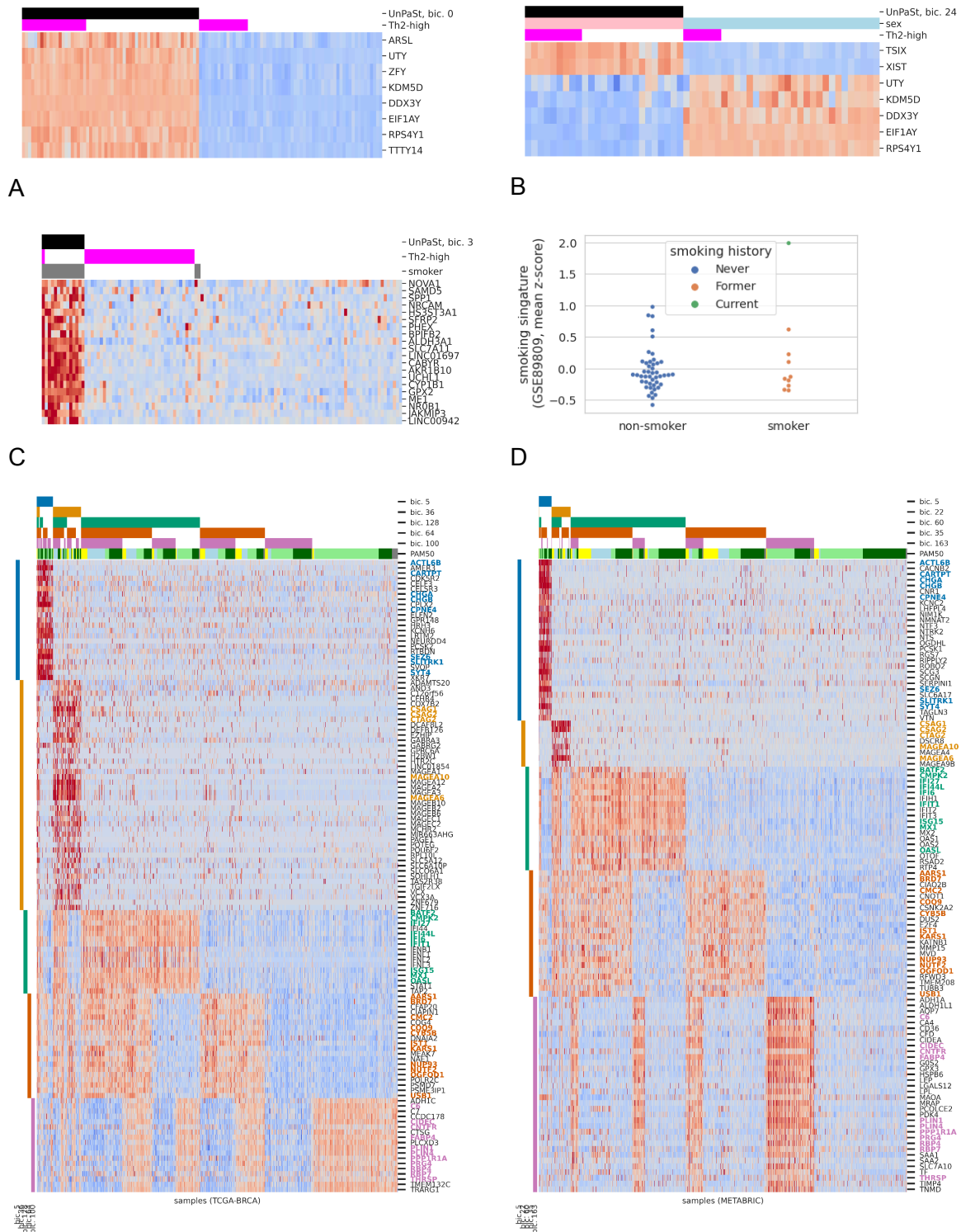


Figure 5. The examples of similar biclusters found by UnPaSt in independent datasets. Two biclusters composed of genes with sex-specific expressions identified in the GSE4302 (A) and GSE89809 (B) datasets. Sample membership in the biclusters and in Th2-high subgroups are highlighted with black and magenta color bars on the tops of the heatmaps. The sex of the donors was available only for the GSE89809 data and therefore is shown in panel B only. C. A 20-gene bicluster found in the GSE4302 dataset with overrepresentation of samples obtained from smoking individuals (shown with the gray color bar). D. Mean z-scores of 20 genes associated with smoking in the GSE89809 cohort. The only sample obtained from a current smoker overexpresses this 20-gene signature higher than any other sample in the cohort. E. Five pairs of the most similar biclusters found in TCGA-BRCA and

METABRIC datasets by UnPaSt matched based on the similarity of their gene sets. Matched biclusters are highlighted with bars of the same color and shared genes are highlighted with bold text font. Blue - neuroendocrine, orange - cancer antigens, green - interferon response, red - immunoproteasome, purple - adipocytes & adipogenesis.

Other aspects of method performance

Biclustering methods that have demonstrated superior performance in unsupervised patient stratification tasks are solving computationally more complex problems than conventional clustering and factorization methods. Therefore, we also compared UnPaSt against other biclustering methods in terms of their running time and peak memory consumption. Because some biclustering methods produce many strongly overlapping biclusters, we also estimated the redundancy of the resulting bicluster sets.

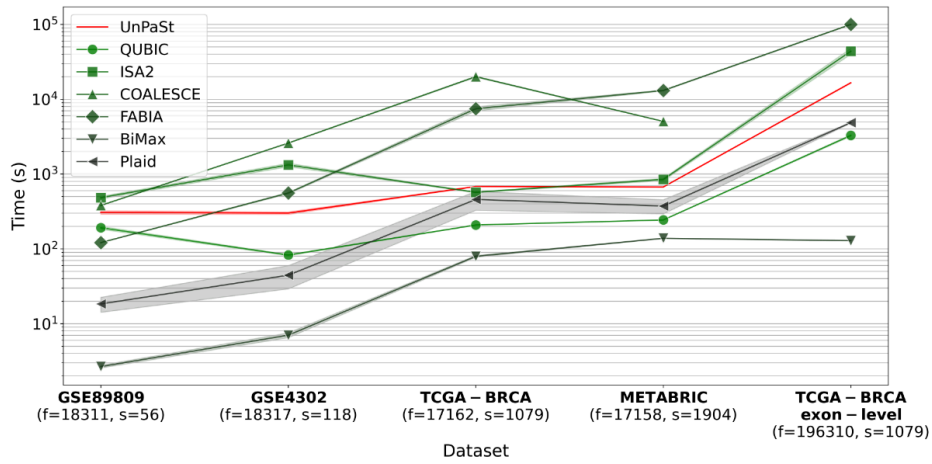
Runtime and memory requirements

The performance of UnPaSt and other biclustering methods in terms of running time and memory requirements was evaluated on four expression datasets comprising 17,158 - 18,317 features and 56 - 1904 samples. To assess the effect of increased number of features on computational costs, a fifth dataset including 196,310 exon-level expression profiles of 1079 TCGA-BRCA samples was added to this benchmark. UnPaSt has demonstrated reasonable running time (from 4min 47s to 11min 28s for gene expression datasets and up to 4h 39min for exon-level expression data on a server with 56 cores at 2,70GHz and 504GB of RAM available) and peak memory consumption (130MiB - 4.29GiB), comparable to other biclustering methods (Figure 6A-B), and with an on average longer runtime but rather low memory footprint compared to clustering and factorization methods (Supplementary Figure S8).

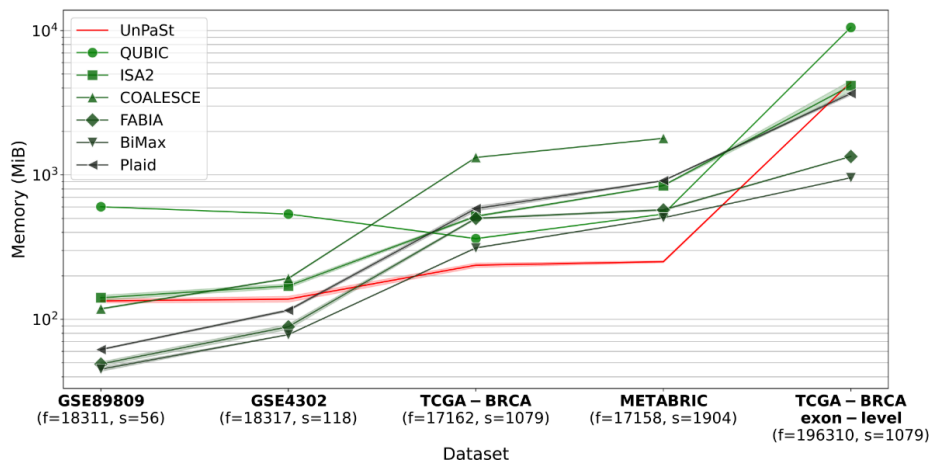
Redundancy

Some biclustering methods tend to generate large and highly redundant sets of biclusters, where numerous strongly overlapping biclusters might match with one pattern with little variations. This redundancy creates a serious obstacle for the user, since it increases the problem of multiple testing and may lead to an inadequate assessment of the method's performance. To assess the redundancy of outputs produced by UnPaSt and other biclustering methods, we computed the fractions of significantly matching pairs of biclusters among all possible bicluster pairs (Figure 6C). A pair of biclusters was considered to be significantly matching, if the size of their overlap in features and samples was significantly larger than expected by chance (adjusted p-value < 0.05, chi-squared test). UnPaSt generated the least redundant set of biclusters, while most of its competitors output plenty of highly overlapping biclusters.

A



B



C

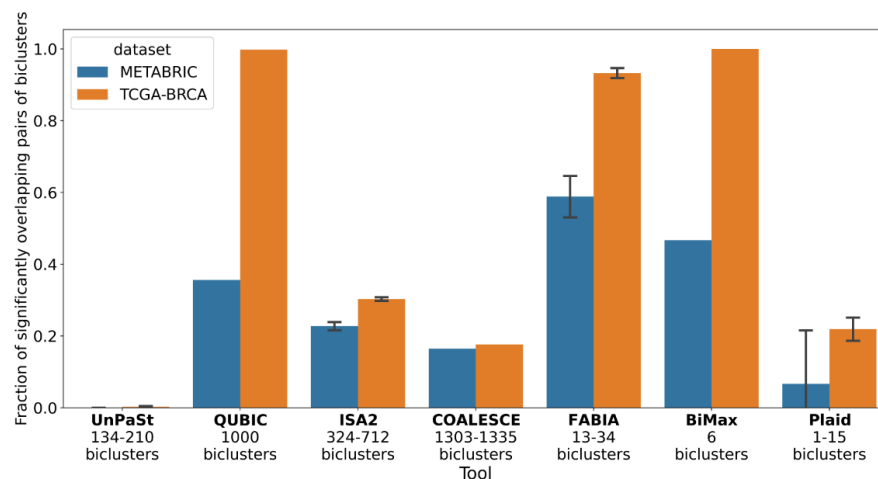


Figure 6. Running time (A) and peak memory consumption (B). Running time and peak memory consumption of biclustering tools applied to five real-word expression datasets of various sizes regarding features and samples. Error areas around lines show the standard deviation in runtime and memory consumption in five runs of non-deterministic methods. It is noteworthy that UnPaSt's runtime and memory

consumption grow slowly with the sample size but is more heavily influenced by the number of features (red line) opposed to for example FABIA, for which both dimensions seem to increase memory and time consumption. COALESCE could not be evaluated on the exon-level expression case, because of an error in the input preprocessing step of the execution suite JBiclustGE due to the large number of features. **C. Redundancy analysis of biclustering results.** The 'Fraction of Significant Pairs' (FSP) metric is utilized to estimate the uniqueness of the biclusters produced by each method, calculated pairwise for all biclusters generated. For non-deterministic methods, each case (METABRIC, TCGA-BRCA) and algorithm pairing was executed five times to assess fluctuations in the generation of overlapping biclusters, depicted by the standard deviation bars. UnPaSt demonstrates a commendable balance between stability (over multiple replication runs), opposed to for example Plaid, while avoiding redundancy, generating a significant number of diverse biclusters without producing many similar results. This is indicated by its comparably small error bars, hinting towards a rather consistent performance across different runs.

Applications to other omics and multi-omics data

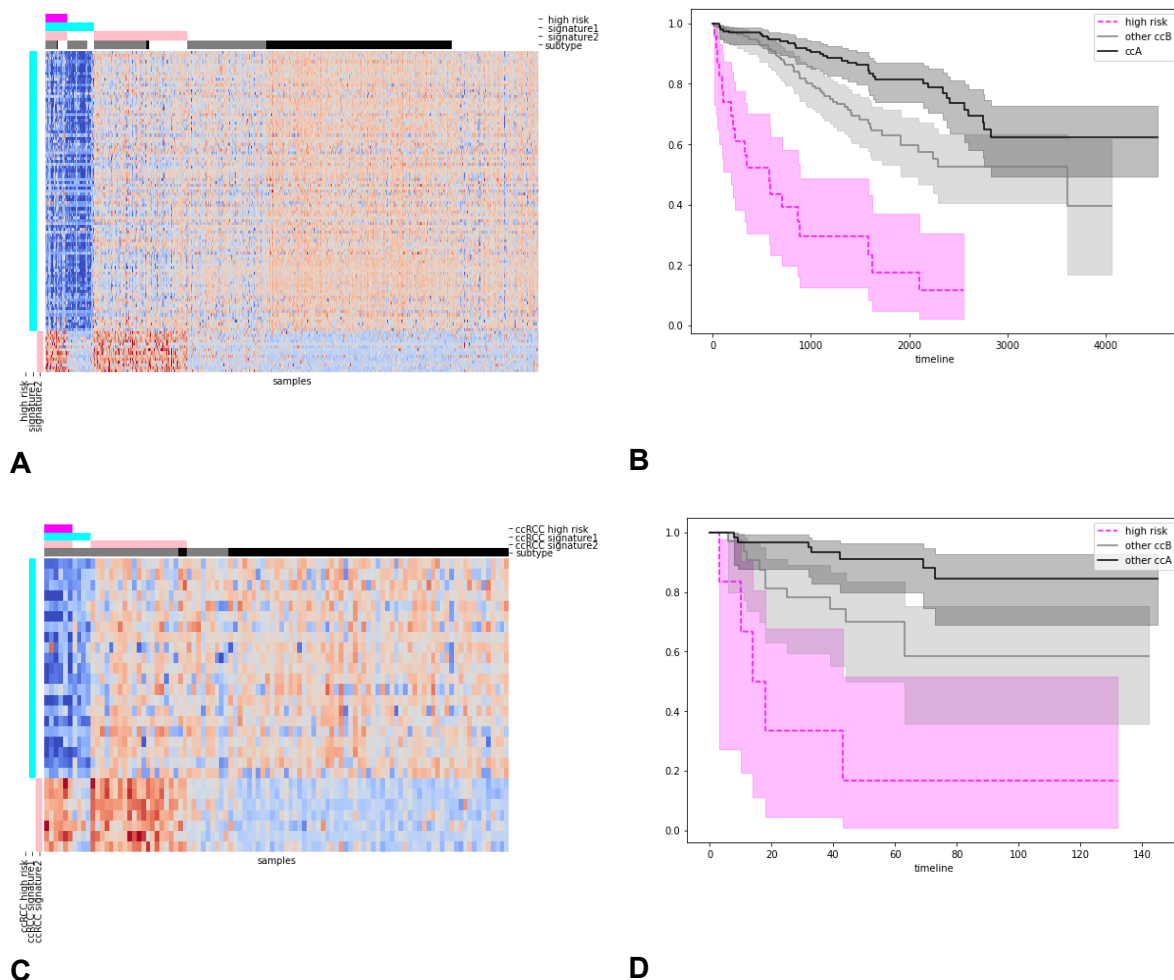


Figure 7. UnPaSt identifies reproducible OS-associated expression signatures in kidney cancer in the TCGA-KIRC⁶⁵(**A,B**) and (E-MTAB-1980⁶⁶) cohorts (**C,D**), which define a high-risk patient subgroup. The heatmaps on panels **A** and **C** show normalized expressions of signature1 (blue), and signature2 (pink) genes in the TCGA-KIRC and E-MTAB-1980 cohorts respectively, black and gray color bars highlight ccA and ccB molecular subtypes. Both signatures represent subsets of previously described molecular subtype ccB (gray), known to have a reduced overall survival compared to ccA subtype (black)⁶⁷. A subset of samples expressing both expression signatures (magenta) demonstrates statistically significantly reduced overall survival in both cohorts, when compared to the rest of patients with ccB (**B,D**).

Discussion

In this study, we benchmarked 23 methods for unsupervised patient stratification on multiple real and simulated datasets. Our results confirmed that most stratification methods achieve high performance in scenarios with well-differentiated non-overlapping sample clusters. In such scenarios, computationally complex factorization methods, whose popularity has been growing in recent years, may be even slightly inferior in terms of performance compared to conventional clustering methods, let alone running time and memory consumption. However, conventional clustering methods struggle to find correct sample clusters when they can overlap, or get obscured by other patterns or noise in the data.

To eliminate this deficiency, we developed UnPaSt, a novel method for unsupervised patient stratification based on biclustering. Unlike its competitors, UnPaSt was efficient in all scenarios, and detected patterns of various kinds, from frequent and strongly differentially expressed signatures defining Luminal and Basal breast cancer subtypes, to smaller signatures consisting of only several biomarkers (e.g. Th2-high asthma, sex-specific gene expression, smoking signature), or signatures corresponding to rare disease subtypes (e.g. breast cancer with neuroendocrine differentiation). This sensitivity to patterns defined by a small number of features makes UnPaSt a promising tool for exploration of diseases with molecular subtypes defined by few specific biomarkers which are harder to distinguish than e.g. breast cancer subtypes.

Furthermore, we investigated the influence of parameter settings on method performances. Our results revealed that many factorization and biclustering methods parameters are sensitive to the choice of parameters and may underperform with default settings. Nevertheless, most of these methods do not provide guidelines for parameter selection and do not perform automatic parameter tuning, leaving it to the user. This is a significant drawback, considering that in real-world scenarios, adequate parameter tuning in the absence of ground truth is challenging, and repeated algorithm execution is computationally demanding. UnPaSt emerges as a practical solution as it does not require the user to specify the expected number of clusters, and robustly demonstrates high performance with varying parameters on test data (Figure S3), as well as with default parameters across multiple datasets (Figure 7 and Supplementary Text).

The outstanding performance of UnPaSt in real and synthetic data benchmarks is attributed to two factors: (i) it reduces the patient stratification problem to a biclustering problem, which enables the discovery of overlapping sample sets, and (ii) its feature selection procedure aims specifically at feature subspaces, in which the whole sample cohort can be divided into two distinct subsets with high and low abundance of corresponding features. In other words, the problem solved by UnPaSt can be understood as an unsupervised version of differential expression analysis problem, where target class labels are not known a priori and are to be found. Although UnPaSt does not guarantee that the discovered biclusters exhibit statistically significant differential expression, this hypothesis can be tested for each discovered bicluster by any state-of-the-art differential expression analysis method, e.g. *limma*⁴⁹.

Besides rigorous testing of UnPaSt on transcriptomic data, we also demonstrated its utility for analyzing other types of biological data, including multi-omics. We have shown that

UnPaSt goes beyond the largest non-overlapping patterns visible for traditional clustering methods and provides a more comprehensive overview of data heterogeneity. This not only makes UnPaSt a promising alternative to existing clustering and data integration methods but also highlights its potential as a feature selection and dimensionality reduction technique. UnPaSt biclusters only the features delineating sample subpopulations, while excluding the rest. In this way, it selects the features that are potentially the most informative for machine learning models and represent promising biomarker candidates. Each differentially expressed bicluster detected by UnPaSt integrates a group of features that define the same sample clusters. Thus, a biclustering result can be viewed as an interpretable lower-dimensional representation of a multidimensional dataset.

Supplementary data

Methods

Simulated data

To analyze the behavior of the methods under different circumstances, we defined three scenarios with increasing complexity and varied the number of subtype-specific features from 500 to 50 and 5 in each scenario. This resulted in nine 10000-feature matrices (3 scenarios x 3 feature set sizes) simulating omics data derived from a cohort of 200 patients classified into four subtypes. Samples of each dataset were randomly assigned to four subtypes, including 10, 20, 50, or 100 samples. In scenario A, simulated subtypes were mutually exclusive, i.e. each sample belonged to no more than one subtype. In scenarios B and C, samples were assigned to each subtype independently, and subtypes overlapped in samples, i.e., each sample was assigned to 0-4 subtypes. First, each matrix was filled with values drawn from a standard normal distribution simulating the background. Second, four non-overlapping sets of $n = 5, 50, 500$ features were randomly chosen to represent subtype-specific biomarkers. Third, for each subtype, values corresponding to subtype-specific genes were replaced with the values drawn from $\mathcal{N}(4, 1)$. Finally, in scenario C, four co-expression modules not associated with target subtypes and containing 500 features were added to the background. To add each co-expression module, we sampled 500 background features and modified all feature vectors f_i except the first one as

$f'_i = f_0 r + f_i \sqrt{1 - r^2}$, where $i = 1 - 499$, and $r = 0.5$ to establish Pearson's correlations between features from one module to be around 0.5.

Data preprocessing

RSEM-normalized and log2-transformed gene-level read counts, exon-level expressions, and sample information for TCGA-BRCA cohort¹ were obtained from XENA⁶⁸ TCGA Pan-Cancer (PANCAN) data hub ([https://xenabrowser.net/datapages/?cohort=TCGA%20Pan-Cancer%20\(PANCAN\)](https://xenabrowser.net/datapages/?cohort=TCGA%20Pan-Cancer%20(PANCAN))). Out of 1108 samples in the TCGA-BRCA cohort, 1079 samples obtained from primary tumors of females and 29999 genes with at least 3 normalized read counts in at least 5 samples were kept. Normalized and log2-transformed expressions of 24368 genes in 1904 samples and clinical data from the METABRIC cohort⁵⁷ was downloaded from cBioPortal^{69,70} (https://www.cbioportal.org/study/summary?id=brca_metabric). To simplify the comparison

and validation of findings in METABRIC and TCGA-BRCA, 17162 genes presented in both datasets were kept. RPKM exon-level expressions of the 1079 samples from the TCGA-BRCA cohort were log₂-transformed, and exons with less than ten values larger than one were excluded, resulting in 196310 features.

Raw .CEL files and sample annotations for GSE4302⁷¹ and GSE89809⁵⁸ datasets were obtained from NCBI GEO⁷² database (<https://www.ncbi.nlm.nih.gov/geo/>). Only bronchial epithelium samples were included in the analysis. Raw files were downloaded, read, background-corrected, RMA-normalized, and log₂-transformed using R packages *GEOquery* 2.54.1⁷³, *affy* 1.64.0 and *affyio* v1.56.0⁷⁴. Probe IDs were mapped to gene names using *biomaRt*⁷⁵ v2.42.1 and probes with maximal variance were selected per gene using *collapseRows()* function from the *WGCNA*⁴⁶ v1.70-3 R package.

Identification of known molecular subtypes in breast cancer and asthma

Unlike in the TCGA-BRCA dataset, in METABRIC the claudin-low subtype was treated as the sixth mutually exclusive subgroup not overlapping with any PAM50 subtype, to unify sample classifications in TCGA-BRCA and METABRIC datasets. Therefore, we re-assigned subtype labels using supervised classifiers from *genefu* (<https://bioconductor.org/packages/release/bioc/html/genefu.html>) R package v2.18.1. Expression profiles from TCGA-BRCA and METABRIC datasets were classified into Luminal A, Luminal B, HER2-enriched, and Normal-like subtypes using the *molecular.subtyping()* function with `sbt.model = "pam50"`. In agreement with *Fougner et al.*⁵², we considered claudin-low as an additional phenotype independent from PAM50 classification and subdivided all samples into claudin-low merged with PAM50 classification and non-claudin-low subsets regardless of their PAM50 labels using *claudinLow()* function. Luminal, Basal, and HER2-enriched subtypes predicted by supervised classifiers closely resembled published classification, while the assignment of samples into Luminal A and B subsets in both datasets, and into Normal-like in METABRIC differed (Supplementary Figure S6).

Th2-high asthma subgroups in GSE4302 and GSE89809 cohorts were identified using the same approach as described by Woodruff et al.². In each cohort, samples were separated into two groups based on the expressions of three biomarkers, POSTN, SERPINB2, and CLCA1 using hierarchical clustering (Python *scikit-learn* v.1.2.2) with complete linkage and Euclidean distance. This resulted in 37 out of 118 (31%) and 15 out of 56 samples (27%) classified as Th2-high in GSE4302 and GSE89809 cohorts respectively.

Method execution

Each method was tested with default parameters and grid search for parameter tuning, on both the simulated and the breast cancer data (Supplementary Table S1). For non-deterministic methods, each parameter combination was executed five times.

For the assessment of running time and memory consumption, each method was executed sequentially on a server, equipped with 504GB of memory and a 56-core CPU operating at 2.70 GHz. Same as before, each non-deterministic method was executed five times.

Biclustering methods BiMax, FABIA, ISA2, Plaid, and QUBIC were executed using MoSBI⁷⁶ v1.10.0 (R 4.2.1) and COALESCE using JBiclustGE-CLI⁷⁷ v1.0.0 (Java 8).

Performance evaluation

Comparing sample clusterings with ground truth sample sets

Evaluating the performance of clustering and biclustering methods on real data is a challenging task for several reasons. First, standard clustering comparison metrics such as adjusted Rand index (ARI) or mutual information are only suitable for the comparison of partitions consisting of non-overlapping clusters, while some methods output heavily overlapping sample sets. Second, biological and technical variation introduces patterns in real data unrelated to the target disease. While these variations veil the disease pattern, they also mislead clustering algorithms and lead to a high rate of false positives which has to be accounted for in the evaluation metric to estimate method performance accurately. Third, the average number of clusters and the distribution of cluster sizes widely varies across evaluated methods, spanning the range from several clusters to thousands. Therefore, to minimize the contribution of predicted clusters that match known clusters just by chance, it is necessary to consider the statistical significance of the observed matches between predicted and known clusters.

To avoid these pitfalls, we propose to use the weighted sum of ARIs for the statistically significant best matching pairs of predicted and ground truth clusters defined by established molecular classifications, like PAM50. Among predicted sample clusters, best matches of ground truth clusters are identified based on significance of their overlap.

Let S be a set of all samples in the cohort, and clustering $C_{true} = \{C_{t_1}, \dots, C_{t_m}\}$ represents an established molecular classification with m disease subtypes that can overlap. To identify the best matches of each known subtype $C_{t_i} \in C_{true}$ among n predicted sample clusters $C_{pred} = \{C_{p_1}, \dots, C_{p_n}\}$, the three following steps are performed.

1. For each pair of known and predicted clusters C_{t_i} and C_{p_j} , the statistical significance of the overlap is assessed with Fisher's exact tests and the lowest two-tailed p -value is stored. If the right-tailed p -value exceeds the left-tailed p -value suggesting that C_{p_j} samples are under-represented in C_{t_i} , C_{p_j} is inverted: $C_{p_j} := S \setminus C_{p_j}$. When all overlaps are tested, resulting p -values p_{t_i, p_j} are adjusted for multiple testing using Bonferroni method.
2. For each ground truth cluster C_{t_i} , the predicted clusters which most specifically match C_{t_i} and not any other true cluster $C_{t_k \neq i} \in C_{true}$ (i.e. having the lowest p -value) are considered to be the best match candidates of C_{t_i} .
3. For each of the best matching candidates of C_{t_i} where the adjusted p -values remain below the user-defined threshold (e.g. 0.05, as set in this work), the cluster C_{p_j} with the highest ARI with C_{t_i} is chosen as its best match.

When best matches are identified for all $C_{t_i} \in C_{true}$, overall performance is computed as sum of their ARI weighted proportionally to the size of C_{t_i} :

Performance = $\sum_i^m ARI(C_{t_i}, C_{p_j})w_{t_i}$, where $w_{t_i} = \frac{|C_{t_i}|}{\sum_i |C_{t_i}|}$, and C_{p_j} having the highest ARI across all candidates from C_{pred} significantly overlapping C_{t_i} .

Redundancy of biclusters

During the systematic evaluation of other biclustering methods and researching their methodology, it was noticed that some methods tend to produce many overlapping or highly similar biclusters. To assess the redundancy of resulting bicluster sets, the following approach was used:

1. All biclustering algorithms were executed on two datasets: METABRIC and TCGA-BRCA, using optimized parameters. These datasets were chosen because optimized parameters for the individual sets had been identified earlier, allowing for the examination of similarity within their best results. Non-deterministic methods were executed five times to infer standard deviations.
2. For each result of a tool, all biclusters were pairwise compared to calculate two-dimensional Jaccard similarity and statistical significance was evaluated using the chi-squared test. Statistical significant similarity was determined and Bonferroni corrected with $\alpha = 0.05$ and m equal to the number of pairwise comparisons in the given result.
3. The primary metric used to assess the uniqueness of bicluster results was the 'Fraction of Significant Pairs' (FSP). This metric is calculated by dividing the number of pairs evaluated to be significantly similar by the total number of all pairwise comparisons for the upper triangle of the full pairwise comparison matrix. The diagonal (identity comparisons) was excluded as they do not provide any significant insight. The total number of comparisons can be denoted as $\binom{b}{2}$ where b is the number of biclusters in a result.

Consensus biclusters

Since UnPaSt is a non-deterministic method, its results obtained in n independent runs with the same input and parameters may vary. To obtain a more stable result and remove poorly reproducible patterns detected only in individual runs, we combine biclusters obtained in multiple runs with the same parameters into consensus biclusters as described below.

1. For every pair of bicluster sets, the pairs of significantly best matching biclusters are identified based on their sample set similarity following the same procedure as was used for matching predicted sample clusters with ground truth and described in the *Performance evaluation* section above.
2. Pairwise similarity matrix for all biclusters detected in n runs was filled with sample-based Jaccard similarities for best matching bicluster pairs or zeroes for all other pairs. Louvain clustering was performed to identify sets of biclusters best

matching each other and the elbow method was applied to select an optimal similarity cutoff from the range of $[J_{min}, J_{max}]$, set to 0.3 and 0.9 respectively in this work.

3. For each group of matched biclusters, the consensus gene set is defined based on the frequencies of each gene appearance. Only genes that are included in at least f of all runs are retained. We set $f = \frac{1}{3}$ to keep genes included in at least two out of five matched biclusters obtained from five independent runs.
4. For each consensus gene set consisting of at least two genes, samples are divided into bicluster and background subsets. For this, the same approach that was used by UnPaSt for feature binarization, is employed.

Statistical analysis

The statistical significance of overlaps between pairs of gene or sample sets was assessed using Fisher's exact test. For the evaluation of bicluster overlaps, the Chi-squared test was used instead of Fisher's exact test. The Python package scikit-learn⁷⁸ (version 1.3.2) was utilized for the computation of test statistics and p-values.

To evaluate the association of a sample cluster or a bicluster with survival, the Cox Proportional Hazards model was employed, adjusting for the donor's age at the time of diagnosis, sex, and tumor stage (where available). Sample membership in a cluster or bicluster, stage, and sex were modeled as binary variables. Time-to-event analysis and plotting of Kaplan-Meier curves were performed using the Python package lifelines (version 0.25.10).

Gene set overrepresentation analysis was performed using clusterProfiler^{79,80} R package (version 3.14.3) and gene sets comprising 5 to 500 genes from GO^{81,82}, DO⁸³, and KEGG^{83,84} and Reactome⁸⁵ databases. In each test, the set of all expressed genes annotated in the database was used as the background. Overlaps passing an adjusted p-value cutoff of 0.05 were considered significant and only overlaps including at least two genes were taken into account.

Differential expression analysis was performed using *limma* 3.58.1 (or *limma-voom* for count data)⁴⁹, upper quartile normalization⁸⁶ from *edgeR* 4.0.16⁷⁹, and genes with $|\logFC| > 1$ and adjusted p-value < 0.05 were considered to be differentially expressed.

In all cases of multiple testing Benjamini-Hochberg procedure⁸⁷ was performed, except for the evaluation of bicluster redundancy analysis where Bonferroni correction was applied instead.

Code availability

The implementation of the UnPaSt algorithm used in this study is publicly available at <https://github.com/ozolotareva/UnPaSt>, along with the code for statistical evaluation of differentially expressed biclusters and for consensus biclustering. For convenience of the users without programming skills, the UnPaSt algorithm can be executed on datasets up to 500 MB via the web server at <https://apps.cosy.bio/unpast/>.

References

1. Liu, J. *et al.* An Integrated TCGA Pan-Cancer Clinical Data Resource to Drive High-Quality Survival Outcome Analytics. *Cell* **173**, 400–416.e11 (2018).
2. Woodruff, P. G. *et al.* T-helper type 2-driven inflammation defines major subphenotypes of asthma. *Am. J. Respir. Crit. Care Med.* **180**, 388–395 (2009).
3. Orange, D. E. *et al.* Identification of Three Rheumatoid Arthritis Disease Subtypes by Machine Learning Integration of Synovial Histologic Features and RNA Sequencing Data. *Arthritis & rheumatology (Hoboken, N.J.)* **70**, (2018).
4. Zheng, C. & Xu, R. Molecular subtyping of Alzheimer’s disease with consensus non-negative matrix factorization. *PLoS One* **16**, e0250278 (2021).
5. Zhang, F. *et al.* Deconstruction of rheumatoid arthritis synovium defines inflammatory subtypes. *Nature* **623**, 616–624 (2023).
6. McCarthy, M. I. Painting a new picture of personalised medicine for diabetes. *Diabetologia* **60**, 793–799 (2017).
7. Schork, N. J. Personalized medicine: Time for one-person trials. *Nature* **520**, (2015).
8. Seyhan, A. A. Lost in translation: the valley of death across preclinical and clinical divide – identification of problems and overcoming obstacles. *Transl. Med. Commun.* **4**, (2019).
9. Brunet, J.-P., Tamayo, P., Golub, T. R. & Mesirov, J. P. Metagenes and molecular pattern discovery using matrix factorization. *Proc. Natl. Acad. Sci. U. S. A.* **101**, 4164–4169 (2004).
10. Yang, Z. & Michailidis, G. A non-negative matrix factorization method for detecting modules in heterogeneous omics multi-modal data. *Bioinformatics* **32**, 1–8 (2016).
11. Zhang, S. *et al.* Discovery of multi-dimensional modules by integrative analysis of cancer genomic data. *Nucleic Acids Res.* **40**, 9379–9391 (2012).
12. Cancer Genome Atlas Research Network. Integrated genomic analyses of ovarian carcinoma. *Nature* **474**, 609–615 (2011).
13. Gao, Y. & Church, G. Improving molecular cancer class discovery through sparse non-negative matrix factorization. *Bioinformatics* **21**, 3970–3975 (2005).
14. Pontes, B., Giráldez, R. & Aguilar-Ruiz, J. S. Biclustering on expression data: A review. *J. Biomed. Inform.* **57**, 163–180 (2015).
15. Padilha, V. A. & Campello, R. J. G. B. A systematic comparative evaluation of biclustering techniques. *BMC Bioinformatics* **18**, 55 (2017).
16. Xie, J., Ma, A., Fennell, A., Ma, Q. & Zhao, J. It is time to apply biclustering: a comprehensive review of biclustering applications in biological and biomedical data. *Brief. Bioinform.* **20**, 1449–1464 (2019).

17. Tini, G., Marchetti, L., Priami, C. & Scott-Boyer, M.-P. Multi-omics integration—a comparison of unsupervised clustering methodologies. *Brief. Bioinform.* **20**, 1269–1279 (2017).
18. Chauvel, C., Novoloaca, A., Veyre, P., Reynier, F. & Becker, J. Evaluation of integrative clustering methods for the analysis of multi-omics data. *Brief. Bioinform.* **21**, 541–552 (2020).
19. Duan, R. *et al.* CEPICS: A Comparison and Evaluation Platform for Integration Methods in Cancer Subtyping. *Front. Genet.* **10**, (2019).
20. Rappoport, N. & Shamir, R. Multi-omic and multi-view clustering algorithms: review and cancer benchmark. *Nucleic Acids Res.* **46**, 10546–10562 (2018).
21. Duan, R. *et al.* Evaluation and comparison of multi-omics data integration methods for cancer subtyping. *PLoS Comput. Biol.* **17**, e1009224 (2021).
22. Leng, D. *et al.* A benchmark study of deep learning-based multi-omics data fusion methods for cancer. *Genome Biol.* **23**, 1–32 (2022).
23. Perou, C. M. *et al.* Molecular portraits of human breast tumours. *Nature* **406**, 747–752 (2000).
24. Neff, R. A. *et al.* Molecular subtyping of Alzheimer’s disease using RNA sequencing data reveals novel mechanisms and targets. *Sci Adv* **7**, (2021).
25. Li, G., Ma, Q., Tang, H., Paterson, A. H. & Xu, Y. QUBIC: a qualitative biclustering algorithm for analyses of gene expression data. *Nucleic Acids Res.* **37**, e101 (2009).
26. Csárdi, G., Kutalik, Z. & Bergmann, S. Modular analysis of gene expression data with R. *Bioinformatics* **26**, 1376–1377 (2010).
27. Hochreiter, S. *et al.* FABIA: factor analysis for bicluster acquisition. *Bioinformatics* **26**, 1520–1527 (2010).
28. Huttenhower, C. *et al.* Detailing regulatory networks through large scale data integration. *Bioinformatics* **25**, 3267–3274 (2009).
29. Prelić, A. *et al.* A systematic comparison and evaluation of biclustering methods for gene expression data. *Bioinformatics* **22**, 1122–1129 (2006).
30. Lazzeroni, L. & Owen, A. PLAID MODELS FOR GENE EXPRESSION DATA. *Stat. Sin.* **12**, 61–86 (2002).
31. Lee, D. D. & Seung, H. S. Learning the parts of objects by non-negative matrix factorization. *Nature* **401**, 788–791 (1999).
32. Zou, H., Hastie, T. & Tibshirani, R. Sparse Principal Component Analysis. *J. Comput. Graph. Stat.* **15**, 265–286 (2006).
33. Argelaguet, R. *et al.* Multi-Omics Factor Analysis—a framework for unsupervised integration of multi-omics data sets. *Mol. Syst. Biol.* **14**, e8124 (2018).
34. Meng, C., Helm, D., Frejno, M. & Kuster, B. moCluster: Identifying Joint Patterns Across Multiple Omics Data Sets. *J. Proteome Res.* **15**, 755–765 (2016).
35. Mo, Q. & Shen, R. iClusterPlus: Integrative clustering of multi-type genomic data. *Bioconductor R package*

- version 1, (2018).
36. Frey, B. J. & Dueck, D. Clustering by passing messages between data points. *Science* **315**, 972–976 (2007).
 37. Roussinov, D. G. & Chen, H. Document clustering for electronic meetings: an experimental comparison of two techniques. *Decis. Support Syst.* **27**, 67–79 (1999).
 38. Zhang, T., Ramakrishnan, R. & Livny, M. BIRCH: an efficient data clustering method for very large databases. *SIGMOD Rec.* **25**, 103–114 (1996).
 39. Ester, M., Kriegel, H., Sander, J. & Xu, X. A density-based algorithm for discovering clusters in large spatial databases with noise. *KDD* 226–231 (1996).
 40. Bar-Joseph, Z., Gifford, D. K. & Jaakkola, T. S. Fast optimal leaf ordering for hierarchical clustering. *Bioinformatics* **17 Suppl 1**, S22–9 (2001).
 41. Scrucca, L., Fraley, C., Brendan Murphy, T. & Raftery, A. E. *Model-Based Clustering, Classification, and Density Estimation Using Mclust in R*. (CRC Press, 2023).
 42. Comaniciu, D. & Meer, P. Mean shift: a robust approach toward feature space analysis. *IEEE Trans. Pattern Anal. Mach. Intell.* **24**, 603–619 (2002).
 43. Shi, J. & Malik, J. Normalized cuts and image segmentation. *IEEE Trans. Pattern Anal. Mach. Intell.* **22**, 888–905 (2000).
 44. Zolotareva, O. *et al.* Identification of differentially expressed gene modules in heterogeneous diseases. *Bioinformatics* **37**, 1691–1698 (2021).
 45. Serin, A. & Vingron, M. DeBi: Discovering Differentially Expressed Biclusters using a Frequent Itemset Approach. *Algorithms Mol. Biol.* **6**, 1–12 (2011).
 46. Langfelder, P. & Horvath, S. WGCNA: an R package for weighted correlation network analysis. *BMC Bioinformatics* **9**, 559 (2008).
 47. Newman, M. E. J. & Girvan, M. Finding and evaluating community structure in networks. *Phys. Rev. E Stat. Nonlin. Soft Matter Phys.* **69**, 026113 (2004).
 48. Zhang, B. & Horvath, S. A general framework for weighted gene co-expression network analysis. *Stat. Appl. Genet. Mol. Biol.* **4**, Article17 (2005).
 49. Ritchie, M. E. *et al.* limma powers differential expression analyses for RNA-sequencing and microarray studies. *Nucleic Acids Res.* **43**, e47 (2015).
 50. Sørliie, T. *et al.* Gene expression patterns of breast carcinomas distinguish tumor subclasses with clinical implications. *Proc. Natl. Acad. Sci. U. S. A.* **98**, 10869–10874 (2001).
 51. Herschkowitz, J. I. *et al.* Identification of conserved gene expression features between murine mammary carcinoma models and human breast tumors. *Genome Biol.* **8**, R76 (2007).
 52. Fougner, C., Bergholtz, H., Norum, J. H. & Sørliie, T. Re-definition of claudin-low as a breast cancer phenotype. *Nat. Commun.* **11**, 1787 (2020).

53. World Health Organization & International Agency for Research on Cancer. *Pathology and Genetics of Tumours of the Breast and Female Genital Organs*. (IARC, 2003).
54. Trevisi, E. *et al.* Neuroendocrine breast carcinoma: a rare but challenging entity. *Med. Oncol.* **37**, 70 (2020).
55. Parker, J. S. *et al.* Supervised risk predictor of breast cancer based on intrinsic subtypes. *J. Clin. Oncol.* **27**, 1160–1167 (2009).
56. Comprehensive molecular portraits of human breast tumours. *Nature* **490**, 61–70 (2012).
57. Curtis, C. *et al.* The genomic and transcriptomic architecture of 2,000 breast tumours reveals novel subgroups. *Nature* **486**, 346–352 (2012).
58. Singhanian, A. *et al.* Multitissue Transcriptomics Delineates the Diversity of Airway T Cell Functions in Asthma. *Am. J. Respir. Cell Mol. Biol.* **58**, 261–270 (2018).
59. Wenzel, S. E. Asthma phenotypes: the evolution from clinical to molecular approaches. *Nat. Med.* **18**, 716–725 (2012).
60. Modena, B. D. *et al.* Gene Expression Correlated with Severe Asthma Characteristics Reveals Heterogeneous Mechanisms of Severe Disease. *Am. J. Respir. Crit. Care Med.* **195**, 1449–1463 (2017).
61. Frøssing, L., Silberbrandt, A., Von Bülow, A., Backer, V. & Porsbjerg, C. The Prevalence of Subtypes of Type 2 Inflammation in an Unselected Population of Patients with Severe Asthma. *J. Allergy Clin. Immunol. Pract.* **9**, 1267–1275 (2021).
62. Forno, E. *et al.* Transcriptome-wide and differential expression network analyses of childhood asthma in nasal epithelium. *J. Allergy Clin. Immunol.* **146**, 671–675 (2020).
63. Hoyer, A. *et al.* The functional role of CST1 and CCL26 in asthma development. *Immun Inflamm Dis* **12**, e1162 (2024).
64. Spira, A. *et al.* Effects of cigarette smoke on the human airway epithelial cell transcriptome. *Proc. Natl. Acad. Sci. U. S. A.* **101**, 10143–10148 (2004).
65. Cancer Genome Atlas Research Network. Comprehensive molecular characterization of clear cell renal cell carcinoma. *Nature* **499**, 43–49 (2013).
66. Sato, Y. *et al.* Integrated molecular analysis of clear-cell renal cell carcinoma. *Nat. Genet.* **45**, 860–867 (2013).
67. Brannon, A. R. *et al.* Molecular Stratification of Clear Cell Renal Cell Carcinoma by Consensus Clustering Reveals Distinct Subtypes and Survival Patterns. *Genes Cancer* **1**, 152–163 (2010).
68. Goldman, M. J. *et al.* Visualizing and interpreting cancer genomics data via the Xena platform. *Nat. Biotechnol.* **38**, 675–678 (2020).
69. Cerami, E. *et al.* The cBio cancer genomics portal: an open platform for exploring multidimensional cancer genomics data. *Cancer Discov.* **2**, 401–404 (2012).
70. Gao, J. *et al.* Integrative analysis of complex cancer genomics and clinical profiles using the cBioPortal. *Sci.*

Signal. **6**, 11 (2013).

71. Woodruff, P. G. *et al.* Genome-wide profiling identifies epithelial cell genes associated with asthma and with treatment response to corticosteroids. *Proc. Natl. Acad. Sci. U. S. A.* **104**, (2007).
72. Barrett, T. *et al.* NCBI GEO: archive for functional genomics data sets—update. *Nucleic Acids Res.* **41**, (2013).
73. Davis, S. & Meltzer, P. S. GEOquery: a bridge between the Gene Expression Omnibus (GEO) and BioConductor. *Bioinformatics* **23**, 1846–1847 (2007).
74. Gautier, L., Cope, L., Bolstad, B. M. & Irizarry, R. A. affy—analysis of Affymetrix GeneChip data at the probe level. *Bioinformatics* **20**, 307–315 (2004).
75. Durinck, S., Spellman, P. T., Birney, E. & Huber, W. Mapping identifiers for the integration of genomic datasets with the R/Bioconductor package biomaRt. *Nat. Protoc.* **4**, 1184–1191 (2009).
76. Rose, T. D. *et al.* MoSBI: Automated signature mining for molecular stratification and subtyping. *Proc. Natl. Acad. Sci. U. S. A.* **119**, e2118210119 (2022).
77. Rocha, O. & Mendes, R. JBiclustGE: Java API with unified biclustering algorithms for gene expression data analysis. *Knowl. Based Syst.* **155**, 83–87 (2018).
78. Pandey, G., Atluri, G., Steinbach, M., Myers, C. L. & Kumar, V. An association analysis approach to biclustering. in *Proceedings of the 15th ACM SIGKDD international conference on Knowledge discovery and data mining* 677–686 (Association for Computing Machinery, New York, NY, USA, 2009).
79. Robinson, M. D., McCarthy, D. J. & Smyth, G. K. edgeR: a Bioconductor package for differential expression analysis of digital gene expression data. *Bioinformatics* **26**, 139–140 (2010).
80. Yu, G., Wang, L.-G., Han, Y. & He, Q.-Y. clusterProfiler: an R package for comparing biological themes among gene clusters. *OMICS* **16**, 284–287 (2012).
81. Ashburner, M. *et al.* Gene ontology: tool for the unification of biology. The Gene Ontology Consortium. *Nat. Genet.* **25**, 25–29 (2000).
82. Gene Ontology Consortium *et al.* The Gene Ontology knowledgebase in 2023. *Genetics* **224**, (2023).
83. Schriml, L. M. *et al.* Human Disease Ontology 2018 update: classification, content and workflow expansion. *Nucleic Acids Res.* **47**, D955–D962 (2019).
84. Kanehisa, M., Furumichi, M., Sato, Y., Kawashima, M. & Ishiguro-Watanabe, M. KEGG for taxonomy-based analysis of pathways and genomes. *Nucleic Acids Res.* **51**, D587–D592 (2023).
85. Milacic, M. *et al.* The Reactome Pathway Knowledgebase 2024. *Nucleic Acids Res.* **52**, D672–D678 (2024).
86. Bullard, J. H., Purdom, E., Hansen, K. D. & Dudoit, S. Evaluation of statistical methods for normalization and differential expression in mRNA-Seq experiments. *BMC Bioinformatics* **11**, 1–13 (2010).
87. Benjamini, Y. & Hochberg, Y. Controlling the false discovery rate: A practical and powerful approach to multiple testing. *J. R. Stat. Soc. Series B Stat. Methodol.* **57**, 289–300 (1995).

